Experimental and numerical characterization of a grounded coplanar waveguide for nanoelectroporation applied to liposomes

Laura Caramazza[1,2] (iD), Alessandra Paffi[1], Micaela Liberti[1,2] and Francesca Apollonio[1,2] (iD)

[1]DIET at Sapienza University of Rome, Rome 00184, Italy and [2]Center for Life Nano Science at Sapienza, Istituto Italiano di Tecnologia, Rome 00161, Italy

Abstract

Electroporation has become a powerful technological platform for the electromanipulation of cells and tissues for various medical and biotechnological applications. Recently, nanoporation based on nanosecond pulsed electric fields (nsPEFs) has gained great attention due to its potential to permeabilize the membrane of small vesicles. Here, the authors propose and characterize, both experimentally and through multiphysics modeling, a grounded coplanar waveguide compliant with the wideband requirements for nanosecond pulses to be used for experiments of drug delivery with liposomes activated by nsPEFs.

Introduction

An earlier version of this paper was presented at the 50th European Microwave Conference and was published in its proceedings where a preliminary experimental characterization of the structure as well as microdosimetric analysis were given [1].

Pulsed electric fields of ultra-short duration and high intensity are known to induce cell membrane electroporation, i.e. an increase of membrane permeability due to a rearrangement of the phospholipid bilayer with a consequent pore formation, that facilitates biomolecules, nucleic acids, peptides, and/or proteins to cross the membrane [2].

Recently, nanoporation based on nanosecond pulsed electric fields (nsPEFs) has gained great attention due to its potential to permeabilize the membrane of small vesicles for drug delivery applications [3–6].

Drug delivery methodologies are becoming more and more interesting strategies for pharmacological therapies; versatile nanocarriers, produced from a variety of materials such as metals and inorganic materials, polymers, but more often lipid compounds [7, 8], are used to carry the specific drug to the target site. The breakthrough is nowadays represented by smart drug delivery, defined as an "on demand" delivery at the cell site, which exploits nanovectors sensitiveness to external stimuli [9]. Among the lipid nanocarriers, liposomes are mostly studied as smart drug delivery carriers [10–13] due to their easy production, high biocompatibility, and versatility.

External pulsed electric fields can represent an excellent "smart actuator" of the release and, as such, are investigated in electrochemotherapy and gene delivery applications [3–6, 14]. In this context, the authors demonstrated that nsPEFs are particularly suitable for these drug delivery applications since they can interact with both cellular and liposomal membranes [5, 6, 14] and can be used as an external trigger, as recently experimentally validated in [3, 4], opening the way to liposome drug delivery systems mediated by nanoelectroporation.

However, when dealing with systems for generating and delivering nsPEFs to a selected target, rigorous care must be taken in the exposure system used for experiments: one specific feature of nsPEFs is related to their extremely short time duration (ns) and consequently their broad frequency content, up to a few GHz, which makes that a wideband exposure system should be preferred [15, 16]. Moreover, the high intensity of nsPEFs (MV/m) propagating along the system demands careful attention in avoiding electrical discharges which may cause performance degradation.

With respect to what presented in [1], in this paper authors fully characterize (both experimentally and through multiphysics modeling) a grounded coplanar waveguide (GCPW) compliant with the wideband requirements for nsPEFs to be used for experiments of drug delivery with liposomes. The use of planar wideband structures as exposure systems was already proposed in the past for real-time electrophysiology applications [17, 18], while grounded coplanar waveguides have been proposed in [19, 20] for *in vitro* applications, and used in [21] for *ex-vivo* experiments of pulsed electric fields of hundreds of ns duration.

Here, the new GCPW system is intended to overcome the limitations of impedance matching often present in current experiments for nanoporation of nanosized liposomes [6], which make use of a standard parallel plate cuvette. In that case, researchers are forced to use a low conductivity medium to enhance the transmitted signal [3]. The new system will permit the use of liposome solutions with a broad range of conductivity values, hence improving the coupling of the electric field with the medium, as recently demonstrated by numerical investigations on liposome nanoporation [5, 14]. In fact, those studies showed that lower electric field intensities were needed to activate liposomes if the external conductivity of the liposome solution was increased.

We characterized such a system to be used as a suitable exposure setup able to generate pulses of 10 ns (rise and fall time of about two ns) with intensities up to 10 kV and to deliver the undistorted nsPEFs to the liposome solution due to the GCPW broadband behavior up to a few GHz. The avoidance of electromagnetic interference with laboratory equipment is guaranteed by the grounded structure. Easy accessibility to the biological sample during experiments is possible thanks to the planar waveguide where the sample is placed over the exposure system [22].

Starting from preliminary investigations shown in [1], here the authors organized the paper as follows. First, the complete numerical characterization of the electric field distribution in GCPW without and with a 400 μl sample holder placed in the middle of the strip is given. Successively, the characterization of the GCPW in the frequency domain is performed both experimentally to evaluate the S_{11} and S_{21} parameters in the absence and presence of the sample holder and numerically to compare the frequency behavior of the empty structure with measurements. The experimental characterization is also performed in the time domain, to study the nsPEFs signal transmitted through the GCPW in the absence and presence of the sample holder filled with five solutions of different conductivities. Specifically, the authors evaluate the signal transmitted as a function of position on the coplanar system (at 3, 6, and 9 cm from the excited port 1) and of voltage (from 4 to 8 kV). Finally, a multiphysics microdosimetric model of liposomes exposed to nsPEFs investigates the induced electrical quantities, the transmembrane potential, and the pore density evolution as a function of the electric field applied and the number of pulses delivered, providing a non-linear dependence of liposome nanoporation on the electric field amplitude.

Materials and methods

Numerical characterization of the GCPW

The GCPW was modeled using the ANSYS HFSS (v. 15.0) software, as presented in previous work [19]. A first analysis was carried out in the time domain with a pulsed signal coming from a 50-Ω feeding coaxial cable excited by a lumped port. The applied signal had a trapezoidal waveform, 10 ns long, with rise and fall time equal to 2 ns, and voltage equal to 1 V (see Fig. 1). The transient solution was sampled every 1 ns.

The GCPW was fabricated on a three-layer RO4003C laminate, the dielectric substrate has permittivity $\varepsilon_r = 3.55$ and a thickness of 1.524 mm. Here, the GCPW has been analyzed alone and with the sample holder used in the experimental characterization. It was modeled as a hollow cylinder of Perspex ($\varepsilon_r = 5.5$) with an internal radius of 5.5 and 1 mm thick wall. The holder was filled with 400 μl of saline solution ($\varepsilon_r = 85$; $\sigma = 0.7$ S/m) and placed on the GCPW, as shown in Fig. 1. The conductivity assigned to the
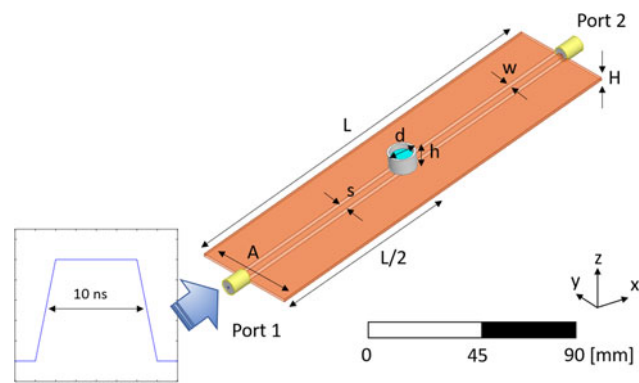
Fig. 1. Geometric model of the GCPW structure used for numerical characterization applying a 10 ns duration pulse.

solution in numerical analysis was one of the intermediate values used for the experimental characterization.

A second analysis with ANSYS HFSS (v. 15.0) software was performed in the frequency domain to evaluate the scattering parameters of the empty structure in the frequency range up to 500 MHz, well above the main lobe of the 10 ns pulse (below 100 MHz).

Figure 1 shows the simulated model with the main geometric parameters: $L = 120$ mm; $A = 50$ mm; $H = 1.524$ mm; $s = 3.35$ mm; $w = 2$ mm; $d = 11$ mm; $h = 8$ mm.

Experimental characterization of the GCPW

A preliminary characterization of the exposure system in the time domain was presented in [1], showing encouraging results in terms of the quality of the signal propagating along the GCPW. In particular, the signal at the output of the generator was measured and results showed a shape similar to the ideal trapezoidal pulse with rise and fall time of 2 ns and a duration of 10 ns (as the duration at half maximum amplitude).

Here, a characterization of the GCPW structure in terms of the scattering parameters was performed with a Vector Network Analyzer (E8363C Agilent), in the frequency range up to 500 MHz, well above the spectral content of 10 ns pulses. Specifically, the set of measurements was performed in the absence and presence of the sample holder filled either with distilled water or with NaCl solution.

Then, a complete and exhaustive characterization of the system was performed using the experimental bench adopted in [1] and briefly reported here in Fig. 2. Figure 2(a) shows the schematics of the setup, Fig. 2(b) shows the setup itself in place, and Fig. 2(c) shows the description of the equipment used as (1) an R&S oscilloscope (RTO2014, Rohde & Schwarz, Germany) to measure and collect the signal in time; (2) a nanosecond pulser (FPG 10-1NM10, FID Technologies, Germany); (3) a high-voltage (HV) coaxial cable and connectors; (4) a couple of HV probes (TT-HV probes 2739, Testec, Germany), able to detect the signal transmitted to the exposure system with a spatial resolution of the field probe of about 1 mm; (5) the exposure system represented by the GCPW; (6) a 50-Ω matching load to close the experimental chain.

In accordance with a measurement procedure used for cuvette exposure system, as in [3, 23, 24], in order to obtain the experimental characterization of the bench, authors have performed the following steps: (i) the GCPW has been fed by the nanosecond
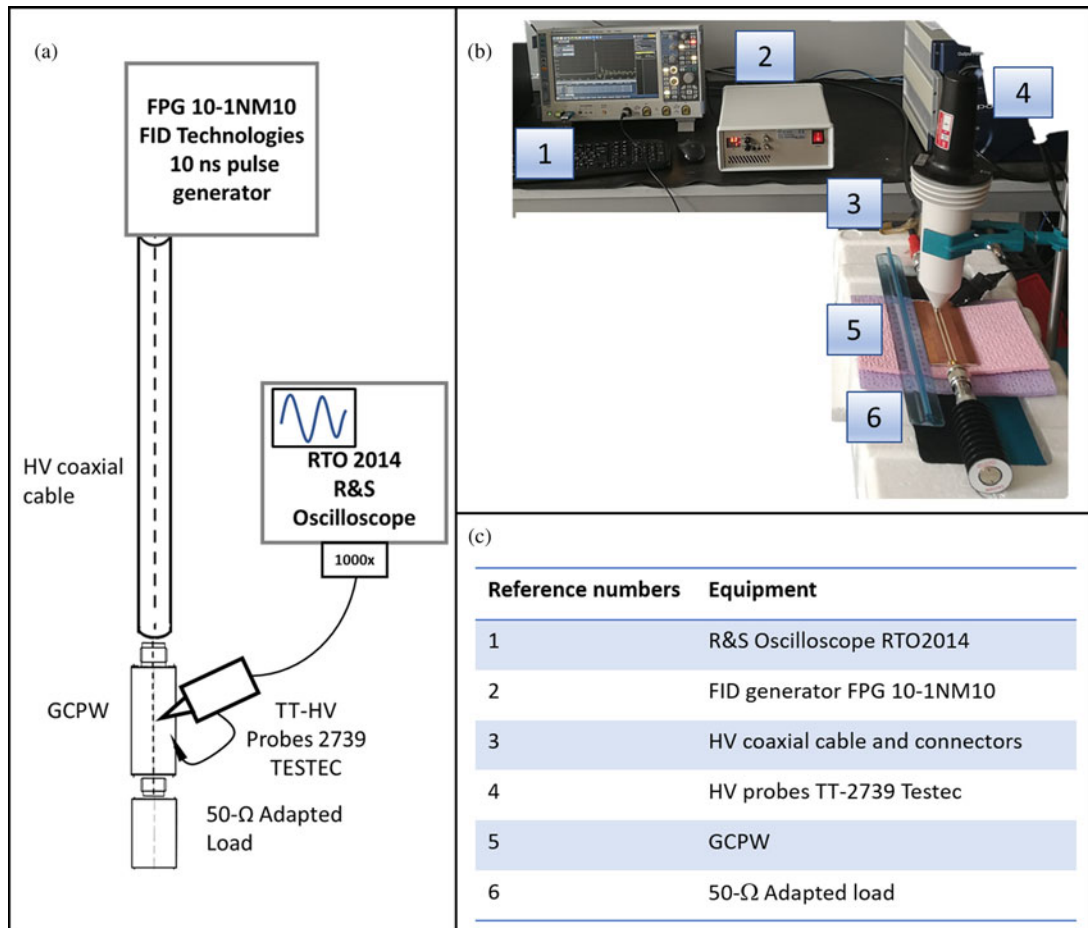
Fig. 2. (a) Scheme of the experimental bench. (b) Experimental bench setup in place. (c) Table of the equipment composing the exposure bench and shown in (b).
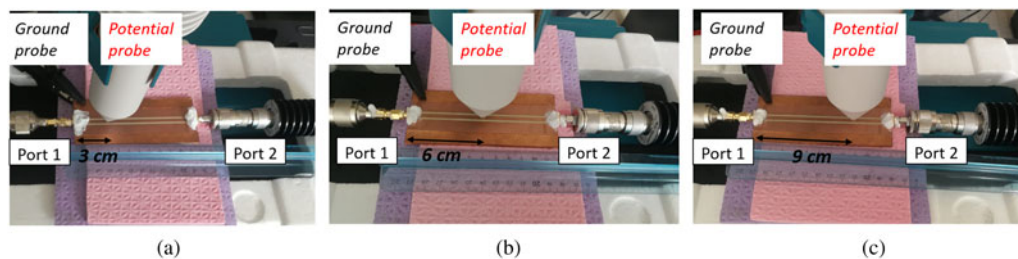

Fig. 3. Detail of the exposure bench during the experimental characterization along the GCPW line, at 3 cm (a), at 6 cm (b), and at 9 cm (c) from port 1.

pulser in a range from 4 to 8 kV to evaluate the transmission of pulses with rise and fall time of 2 ns and a duration of 10 ns; (ii) the signal has been detected along with three positions in the GCPW system, shown in Figs 3(a)–(c), respectively, at 3, 6, and 9 cm from port 1, to evaluate possible distortions; (iii) finally, measurements of the signal inside the Perspex sample holder containing 400 μl solution with conductivity values ranging from 5.6×10^{-4} up to 1.4 S/m, has been done (see Fig. 4). The conductivity values of each solution sample were previously measured using a Precision LCR Meter E4980A from Agilent, as in [3, 6]. This last step has been performed to characterize the exposure system in presence of different host solutions that could contain nanosized lipid vesicles for drug delivery applications.
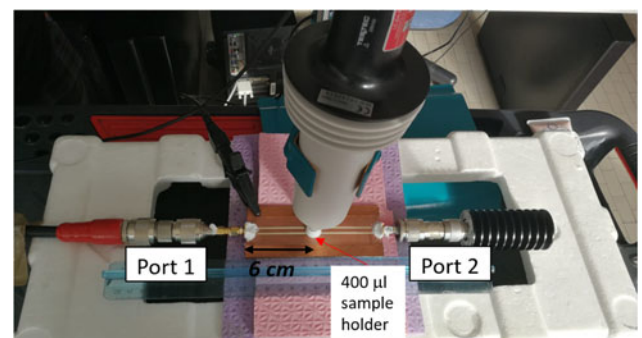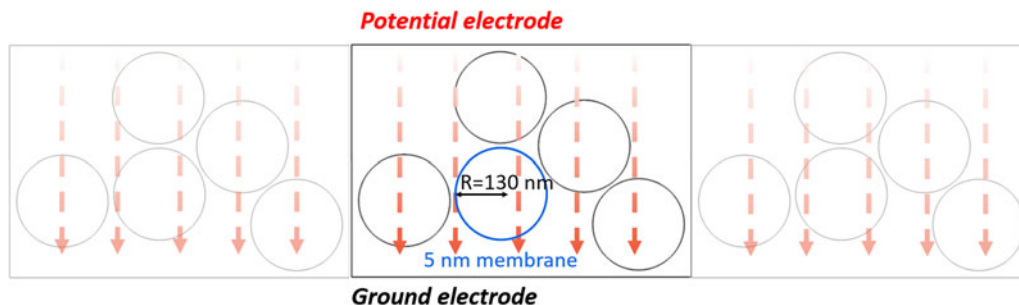

Fig. 4. Detail of the exposure bench during the experimental characterization performed in the presence of a 400 μl sample holder placed at the center of the GCPW line.

Fig. 5. The geometric model used for the microdosimetric study. The model is ideally repeated in space, due to periodic boundary conditions set at the lateral boundaries.

Modeling the electropulsation of nanosized lipid vesicles

To numerically study the feasibility of electropermeabilize lipid vesicles applying a train of nsPEFs, a microdosimetric model has been used with COMSOL Multiphysics v. 5.3. The geometrical model, described for the first time in [1], is composed of five liposomes randomly distributed, characterized by a 130 nm radius, and 5 nm membrane thickness (implemented in the model using a contact impedance setting). Liposomes are placed in a two-dimensional rectangular box representing the external solution, with dimensions of about 1 µm × 0.7 µm. Moreover, in order to simulate a larger geometrical model, periodic conditions were set at the lateral boundaries of the box (see Fig. 5).

In this model, the application of a train of nsPEFs on the distribution of liposomes is simulated considering electric field applied of 8.5, 8.7, 8.8, and 9 MV/m, in order to evaluate the number of pulses that has to be applied to obtain electropermeabilization of liposomes. The pulses are delivered at a repetition frequency of 2 Hz.

To perform this set of simulations, three physics were added to the model using three different modules: (i) the electric currents module from AC/DC mode, to solve the quasi-static electromagnetic problem, (ii) the heat transfer in fluids module, to evaluate possible temperature changes in time, and (iii) the boundary ordinary differential equations and differential-algebraic equations, to study the kinetics of pores on the liposomes membrane, as in [1, 3, 25]. According to the literature, the interaction between lipid vesicles and ultra-short and intense electric fields induces the increase in time of the induced potential across the lipid membrane, known as transmembrane potential (TMP), up to a threshold value, and the simultaneous formation of transient pores across the membrane, determining the consequent increase of membrane conductivity in time. The number of pores is modeled in the literature as a spatial pore density (N) [3, 26–28], whose kinetics depends on the TMP evolution in time with the following equation:

$$\frac{dN}{dt} = \alpha e^{\left(\frac{TMP(t)}{V_{ep}}\right)^2} \left[1 - \frac{N(t)}{N_0} e^{-q\left(\frac{TMP(t)}{V_{ep}}\right)^2} \right] \tag{1}$$

The parameters in equation (1) are reported in Table 1, as in [25].

In accordance with the literature, to obtain the membrane poration, both the TMP and the spatial pore density should overcome their threshold values of 1 V and 10^{14} m^{-2}, respectively.

Usually, unipolar pulses are used in nsPEFs applications, however, some *in vitro* studies experimentally investigated the role of bipolar nsPEFs on the electropermeabilization effect [29, 30]. In this regard, microdosimetric studies could be a powerful tool to

Table 1. Parameters of the pore density kinetics model [25].

Symbol	Value	Description
α [m^{-2} s^{-1}]	10^9	Electroporation parameter
Q	2.46	Electroporation constant
V_{ep} [V]	0.258	Characteristic voltage of electroporation
N_0 [m^{-2}]	1.5×10^9	Equilibrium pore density

understand the phenomena determining the possible decrease of membrane electropermeabilization.

For what concerns unipolar nsPEFs, microdosimetric simulations investigate the effect on the lipid membrane of a single pulse with different durations, determining the electric field value able to porate biological membranes [5, 6, 14]. Recently, in [3, 31] the authors numerically investigated the response occurring when a train of nsPEFs is applied in order to consider possible cumulative mechanisms; the main issue to study such a train is related to a temporal multiscale problem that determines a huge computational cost.

In particular, the pore density kinetics (see equation (1)) [27, 28], describes both pores creation (pulse-ON) and their resealing (pulse-OFF), but the two phenomena occur with two different timescales in the order of ns and s, respectively, for pore formation and pore resealing. This difference in timescale could be considered as a sort of "memory effect" of pore density kinetics and used for electro-stimulate lipid bilayer with a train of nsPEFs with electric field intensity lower than what needed with one single pulse.

Starting from preliminary results reported in [1], the microdosimetric simulations were performed to study liposome nanoporation and pore density kinetics "memory effect" when applying a train of pulses with different electric field amplitudes.

In the model, the conductivity of the solution was chosen as the value of $\sigma = 0.7$ S/m in the middle of the range of experimental conductivity values, in line with the numerical characterization of the exposure system (see "Numerical characterization of the GCPW"). All the physical parameters used in these simulations are reported in Table 2, according to the experimental data and the literature [3–5, 32, 33].

Results

Numerical evaluation of GCPW exposure system with nsPEFs signal

Figure 6 shows the numerical E field distributions for the empty GCPW (Fig. 6a) and inside the solution (Fig. 6b and 6c). All

Table 2. Physical quantities reported in the model to simulate the suspension of liposomes.

Properties of materials	External solution	Membrane	Internal solution
σ [S/m]	0.7	1.1×10^{-7}	0.35
ε_r	85	11.7	85
Cp [J/(kgK)]	4185.5	2000	4185.5
ρ [kg/m³]	993.2	951.1	993.2
k [W/(mK)]	0.62	0.2	0.62

distributions are normalized to the maximum values and calculated on the horizontal xy plane (Fig. 6a and 6c), and on a vertical yz plane passing through the bottom of the sample holder (Fig. 6b). Results shown in Fig. 6 were extracted at the time when the E field reaches its maximum value ($t = 10$ ns).

As evident from Fig. 6(a), the E field is confined in a small region, almost 1 cm wide in correspondence with the two gaps and the central strip. Therefore, to have a homogeneous exposure of the sample, we chose a sample holder with a 5.5 mm radius (Fig. 6(c)). Conversely, despite along the z-axis the E field sharply decays with the distance from the GCPW surface (Fig. 6(b)), a uniform exposure (homogeneity higher than 80%) is achievable if liposomes are placed in a layer on the bottom of the sample holder (Fig. 6(c)).

GCPW experimental characterization results

Scattering parameters of the GCPW are reported in Fig. 7 for the empty structure (simulation solid red curve, measurements dashed red curve), distilled water (dashed green curve), and NaCl solution (dotted magenta curve), in comparison with the spectrum magnitude (solid grey curve) of the nsPEFs signal measured from the generator output. The simulated and measured curves are in very good agreement.

Figure 7(a) shows that the sample solutions worsen the $|S_{11}|$ at 50 MHz from −50 dB (air) to −40 dB and at 500 MHz from −30 to −20 dB, thus indicating that, after all, a very good matching is maintained in the whole range. As shown in Fig. 7(b), the variety of media on the GCPW system does not affect the transmission coefficient $|S_{21}|$ profile in the frequency range up to 1 GHz with values ranging from −0.1 to 0 dB, while the frequency content of the nsPEF signal is mostly confined to frequencies up to 100 MHz.

For what concerns the HV time-domain measurements, Fig. 8 (a) shows the nsPEFs signal measured at 3, 6, and 9 cm from port 1, with an input voltage of 6 kV. The profile in time of the measured voltage is characterized by rise and fall time of about 2 ns and duration of the pulse of 10 ns. Moreover, Fig. 8(b) shows the detected voltage signal in terms of peak value as a function of the input voltage, from 4 up to 8 kV, for all the distances.

The second part of this characterization was performed measuring the signal inside the sample solution, mimicking the final target of an *in vitro* drug delivery application. In this regard, the results are shown in Fig. 9, where the signals are reported as a function of the five different solution samples investigated, each characterized by a different conductivity from 5.6×10^{-4} up to 1.4 S/m, exploring the entire range of possible *in vitro* solution samples, like the ones used in the literature for lipid vesicles [3, 6, 14, 34] and cells [35, 36]. Although the peak values of the

curves reported in Fig. 9 are reduced with respect to the input potential, due to the fact that the measures were performed with the potential HV probe in contact with the insulating bottom of the Perspex sample holder, the signal waveform is maintained for all the solution samples.

Results of the microdosimetric study

In order to give an estimate of the possibility to induce the electropermeabilization of lipid vesicle membranes with the GCPW exposure system, the results of the multiphysics microdosimetric investigation are shown in Fig. 10 for an E field = 8.8 MV/m and applying a train of 10 nsPEFs at the repetition frequency of 2 Hz. Here, we focused on the response of lipid vesicles to the nsPEFs application in terms of induced electric field, current density, and pore density evaluation. In particular, Fig. 10(a) shows the spatial distribution of the current density at $t = 10$ ns for the first applied pulse; this quantity has higher values in the narrow space between liposomes, considering the vesicle–vesicle interaction due to the high density of liposome distribution. Moreover, in Fig. 10(a), the E field is reported as arrows whose size depends on the field magnitude. The arrows show that the presence of liposomes affects the E field direction and focuses it between the vesicles, both enhancing the electrical stimulus on specific vesicles and shielding for other ones. Hence, also the values of the induced TMP in lipid vesicles are affected, as shown in Fig. 10(b) for the first pulse at $t = 10$ ns, together with the arrows of the E field. In accordance with the literature [37], the TMP distribution values are generally lower at the equator and higher at the poles of the vesicles, reaching 1.22 V, slightly above the reference value of 1 V for the beginning of electroporation. Looking at the pore density, which depends on TMP values, it is possible to observe that while this never reaches the threshold of 10^{14} m^{-2} [14] at the first pulse (Fig. 10(c)), the threshold is overcome at the 10th pulse (see Fig. 10(d)) in specific vesicles exhibiting high TMP values. The study of this random distribution of liposomes highlights how the vesicle–vesicle interaction influences the nanoporation. More results on the application of a sequence of intense and ultra-short pulses are given in Fig. 11. Specifically, Fig. 11(a) shows the pore density as a function of the number of applied pulses for different E field intensities: 9 MV/m (yellow circle marker), 8.8 MV/m (green curve), 8.7 MV/m (blue curve), and 8.5 MV/m (red curve). Simulations were stopped either when the poration threshold was overcome or at the applied 20th pulse. A grey dashed line indicates the pore density electroporation threshold of 10^{14} m^{-2} [14, 25]. From the figure, it is possible to observe that, while an E field of 9 MV/m is able to nanoporate the liposomes at the first pulse, six pulses are needed with 8.8 MV/m, and the threshold is not reached during the first 20 pulses for the E field values of 8.7 and 8.5 MV/m. Results of Fig. 11(a) for an applied E field of 8.7 and 8.5 MV/m were fitted with a third-grade polynomial to extrapolate that the minimum number of pulses necessary to nanoporate the liposome solution is, respectively, 29 and 40 pulses, as shown in Fig. 11(b) for all the four E field intensities.

Finally, the number of pulses as a function of the applied E field (Fig. 11(c)) was fitted with a second-grade polynomial to extrapolate the minimum number of pulses necessary to electroporate the liposome solution for a wider range of E field amplitudes, from 9 MV/m down to 1 MV/m. This last curve can be used to plan the number of pulses to be delivered in experiments. Considering, for example, an input from the generator of 8 kV, the
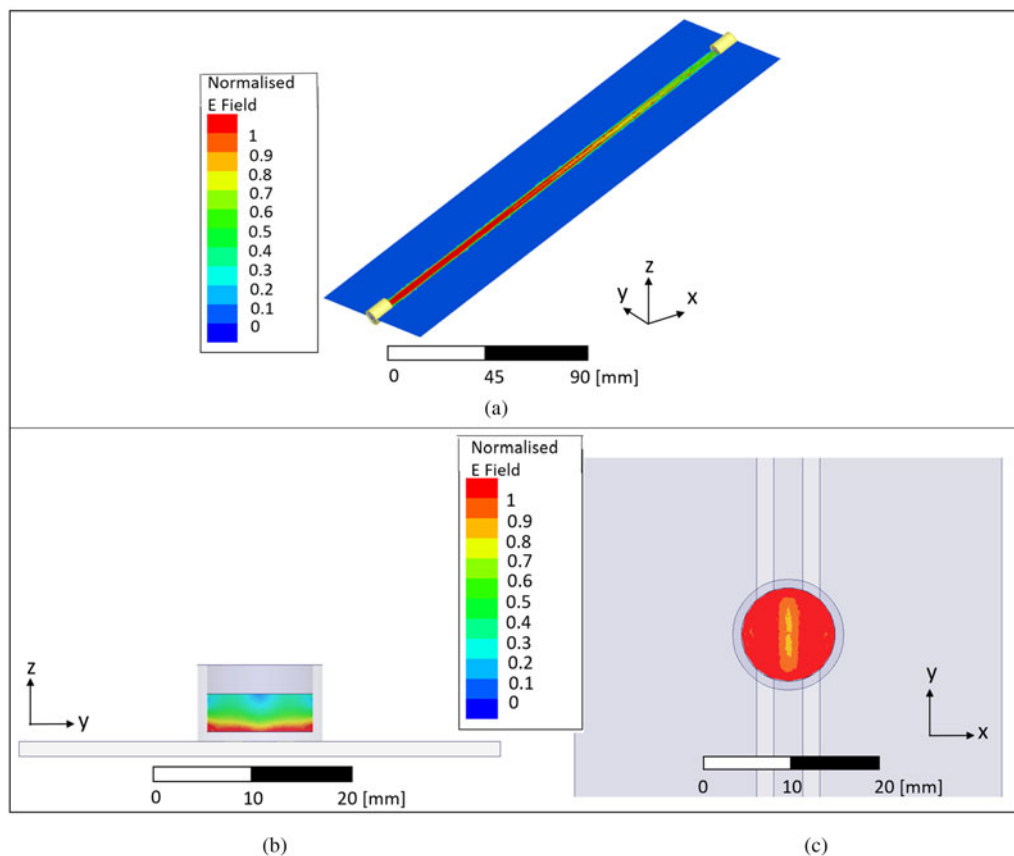
Fig. 6. Results of the numerical simulations. (a) Top view of the GCPW with the E field distribution. (b) Side view of the GCPW with the E field distribution on the central section of the solution sample. (c) Top view of the GCPW with the E field distribution at the bottom of the sample holder.
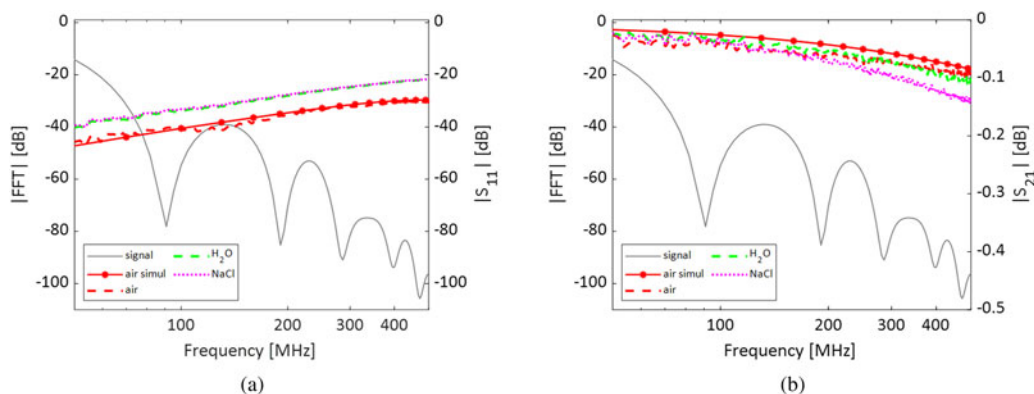

Fig. 7. Results of the scattering parameters $|S_{11}|$ and $|S_{21}|$ simulations and measurements of the GCPW system, respectively, in (a) and (b), in the absence (simulation solid red curve, measure dashed red curve) and the presence of the sample holder filled with distilled water (dashed green curve) and NaCl solution (dotted magenta curve). The solid red curve represents the numerical results of the empty structure. The magnitude of the nsPEF signal spectrum is reported in a grey curve.

potential measured in the exposure system is about 6 kV, and we can estimate an electric field of about 3 MV/m roughly dividing the potential by the 2 mm gap of the structure. In this regard, Fig. 11(c) shows that, due to the highly non-linear profile of the curve, applying a sequence of nsPEFs with 3 MV/m amplitude, around 2000 pulses will be necessary to start electroporation of a solution of nanosized liposomes.

This is in line with what already found in [3], where feasibility experiments on liposome nanoporation were carried out with 2000 nsPEFs delivered at 2 Hz with a maximum electric field of

14 MV/m, using a standard parallel plate cuvette filled with liposome solution with external medium conductivity of 0.03 S/m.

Moreover, in these microdosimetric modeling, temperature changes in liposome solution during nsPEFs application were evaluated. Figure 12 shows the temperature spatial distribution for the E field of 8.8 MV/m, at 10 ns (Fig. 12(a)) and 100 ns (Fig. 12(b)) of the 10th pulse. Here surface arrows describing the gradient of temperature are reported and they underline the effect of lateral boundary conditions as a way to widen the simulation model. The temperature increase during nsPEFs application
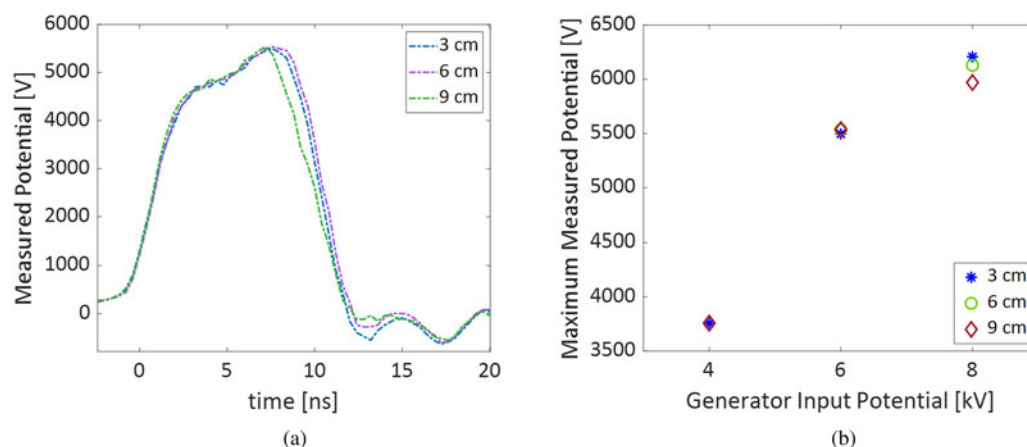
Fig. 8. (a) Nanosecond pulse signal measured in time along the exposure system line, at 3, 6, and 9 cm from port 1, setting the generator at 6 kV. (b) Peak values detected measuring the signal along the exposure system line and setting the input potential from the generator at 4, 6, and 8 kV.
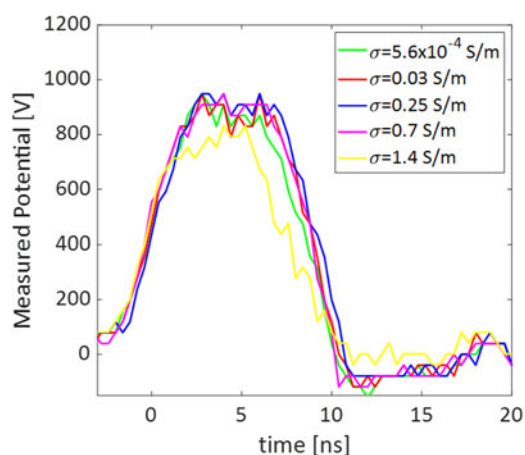
Fig. 9. Signals measured inside the five sample solutions with conductivities from 5.6×10^{-4} to 1.4 S/m and the input voltage of 6 kV.

of about 0.15°C at 10 ns (panel A) is almost totally reduced at 100 ns (panel B) thanks to the heat exchanges with the external environment.

Finally, our results show that, in order to remotely activate nanosized lipid vesicles for drug delivery applications, it is possible to use a train of nsPEFs, choosing the best compromise between the number of pulses and the intensity of the E field applied, with minimal temperature increase.

Discussion

Liposomes as vesicular systems have attracted increasing attention as a means to improve drug delivery systems, due to their possibility to encapsulate both hydrophobic and hydrophilic cargos, to be used in passive and active targeting and to enhance drug bioavailability and therapeutic effects. The new challenge is the possibility to control their delivery by means of nsPEFs hence inducing nanoeletroporation, opening the way to an electromagnetic based smart drug delivery system. In this context, great attention is devoted to systems able to deliver, in an appropriate way, the high intense ultra-short electric field pulse, avoiding distortion of the signal and guaranteeing the proper high intensity along with its propagation. The standard way to deliver nsPEFs to liposome samples is based on two parallel plate cuvettes. In particular, nanoelectroporation as a way to remotely activate lipid vesicles for drug delivery purposes has been recently demonstrated by the authors using a standard cuvette as an exposure system [3]. However, in these cases, particular attention has to be given to the transition between the cuvette and the feeding coaxial cable. Moreover, in the case of such standard sample holders, only liquid solutions with very low values of conductivity can be used, due to reflections coming from the load impedance dependence on the solution conductivity. Conversely, results on numerical investigations of nanoporation of lipid vesicles suggest the use of higher conductivity solutions to easily permeabilize the lipid membrane with lower electric field amplitudes [5, 6, 14].

Wideband GCPW, such as the one presented in this paper, represents a good choice for nsPEFs exposure systems devoted to applications of liposome nanoporation, overcoming the limitations of impedance matching of standard parallel plate cuvette [6]. The system preserves in a good way signal integrity, even when using the highest intensities. Moreover, the system is able to expose liquids of different conductivity values with a wide range of variability, mimicking the ones commonly used as a buffer for liposome solutions. The multiphysics modeling supports the outcome that the threshold for poration of liposome membrane is overcome for at least one pulse of 9 MV/m and a train of six pulses of 8.8 MV/m and a curve of the minimum number of pulses to nanoporate is provided as a function of the E field intensities; this suggests that the present system is good to be used for liposome application looking at the best compromise between nsPEFs train length and pulse amplitude. The numerical results of temperature changes suggest that heat transfer occurs due to nsPEFs application, but thanks to the ultra-short duration of each pulse and the low pulse repetition frequency, heat exchange with the environment can take place.

Conclusion

This work provides a complete characterization of an exposure system to be used for delivering nsPEFs to a target made from a solution of lipid vesicles. A numerical simulation in the time of the exposure system demonstrates that the transmission of
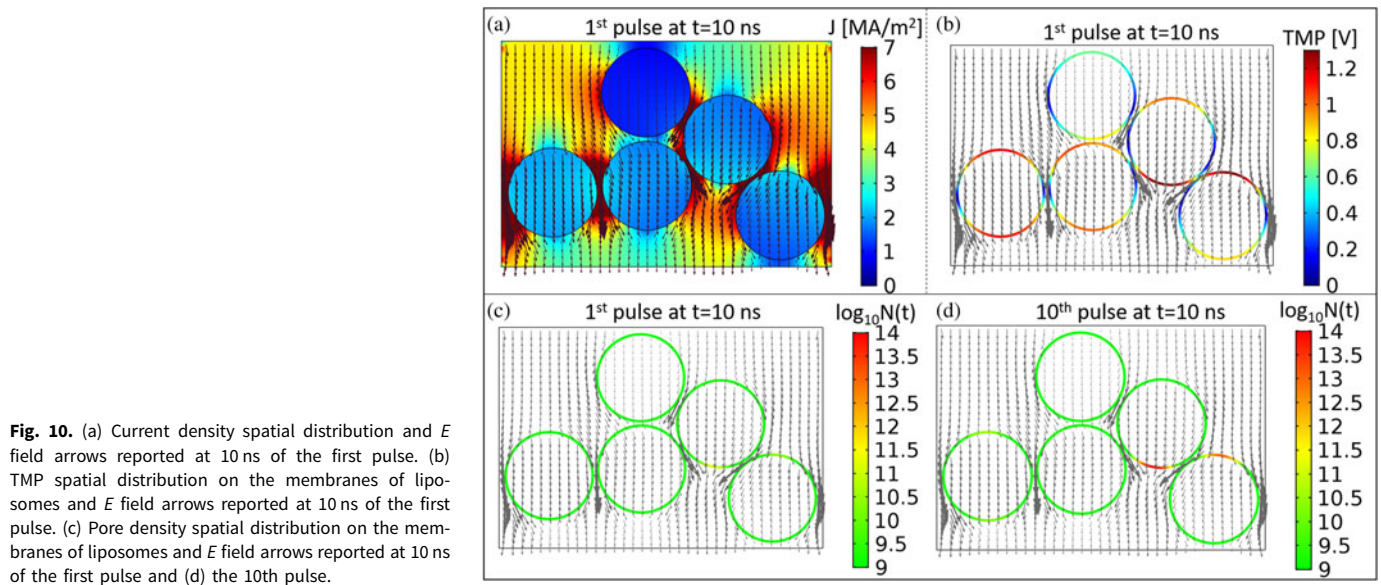
Fig. 10. (a) Current density spatial distribution and *E* field arrows reported at 10 ns of the first pulse. (b) TMP spatial distribution on the membranes of liposomes and *E* field arrows reported at 10 ns of the first pulse. (c) Pore density spatial distribution on the membranes of liposomes and *E* field arrows reported at 10 ns of the first pulse and (d) the 10th pulse.
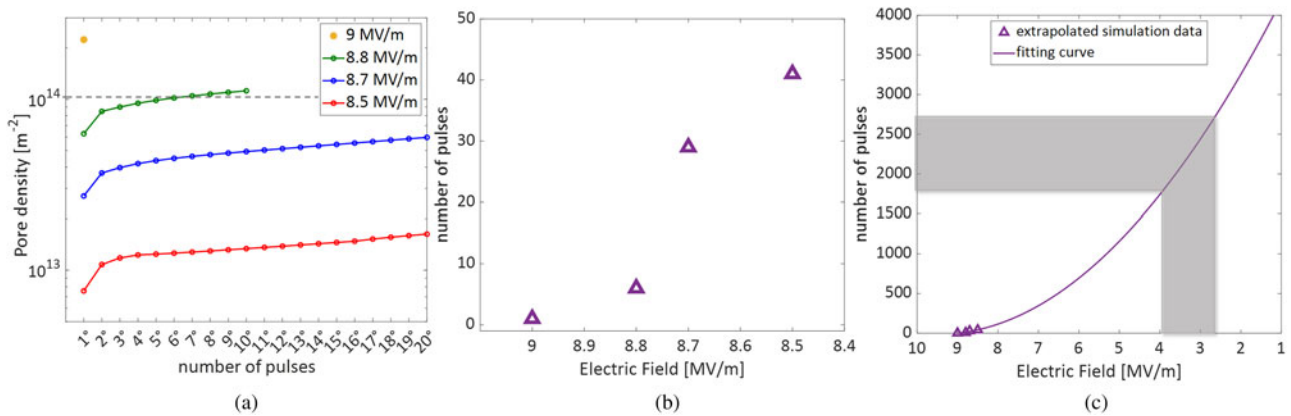
Fig. 11. (a) Evolution of the pore density profile in log scale reported at every 10 ns for a train up to 20 pulses. The pore density threshold is reported as a grey dashed line. (b) The minimum number of pulses to nanoporate liposomes as a function of the *E* field intensities investigated. (c) Simulation data of the minimum number of pulses to nanoporate liposomes (violet triangle markers) reported together with the second-grade fitting curve ($R^2 = 0.8995$).
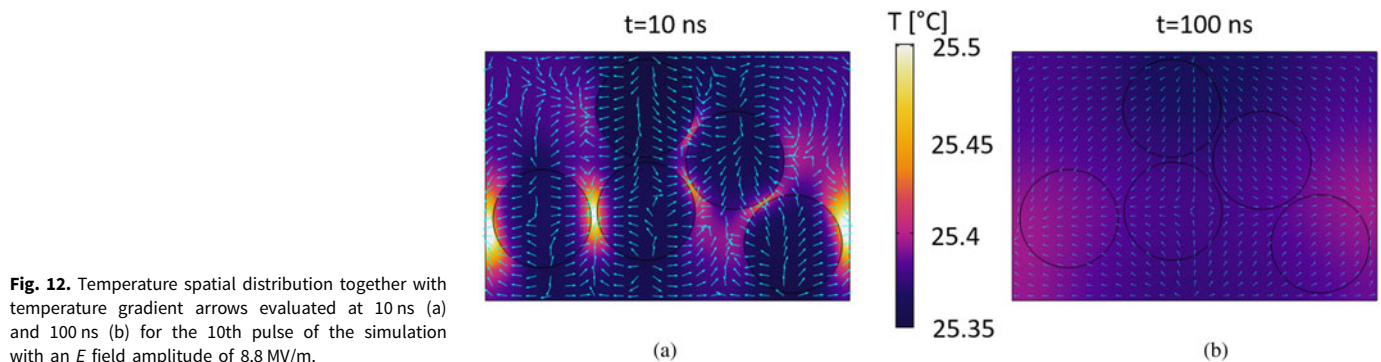
Fig. 12. Temperature spatial distribution together with temperature gradient arrows evaluated at 10 ns (a) and 100 ns (b) for the 10th pulse of the simulation with an *E* field amplitude of 8.8 MV/m.

the *E* field is homogeneous along the system, as expected. Moreover, from numerical outcomes, we provide that it is possible to use this structure to expose liposome samples to a homogenous *E* field generated by the application of nsPEFs signal.

A full experimental and numerical characterization of the entire laboratory bench is proposed, considering the absence and the presence of a solution sample, mimicking an *in vitro* experimental condition, in a wide range of solution conductivities.

Finally, a microdosimetric study is proposed to numerically evaluate the response of liposome suspension as drug delivery systems. The microdosimetric results give an estimate of the possibility of nanoelectroporate liposomes modulating E field intensity and many pulses.

References

1. **Caramazza L, Paffi A, Liberti M and Apollonio F** (2021) A coplanar waveguide system for drug delivery mediated by nanoelectroporation: an experimental and numerical study, 2020 50th European Microwave Conference (EuMC), Utrecht, Netherlands, pp. 999–1002. doi: 10.23919/EuMC48046.2021.9338023.

2. **Kotnik T, Rems L, Tarek M and Miklavčič D** (2019) Membrane electroporation and electropermeabilization: mechanisms and models. *Annual Review of Biophysics* **48**, 63–91.

3. **Caramazza L, Nardoni M, De Angelis A, Paolicelli P, Liberti M, Apollonio F and Petralito S** (2020) Proof-of-concept of electrical activation of liposome nanocarriers: from dry to wet experiments. *Frontiers in Bioengineering and Biotechnology* **8**, 819, 1–14.

4. **Caramazza L, Nardoni M, De Angelis A, della Valle E, Denzi A, Paolicelli P, Merla C, Liberti M, Apollonio F and Petralito S** (2019) Feasibility of drug delivery mediated by ultra-short and intense pulsed electric fields, 41st Annual International Conference of the IEEE Engineering in Medicine and Biology Society (EMBC), Berlin, Germany, pp. 1678–1681.

5. **Denzi A, della Valle E, Apollonio F, Breton M, Mir LM and Liberti M** (2017) Exploring the applicability of nano-poration for remote control in smart drug delivery systems. *The Journal of Membrane Biology* **250**, 31–40.

6. **Denzi A, della Valle E, Esposito G, Mir LM, Apollonio F and Liberti M** (2017) Technological and theoretical aspects for testing electroporation on liposomes. *Hindawi BioMed Research International* **2017**, 5092704, 1–10.

7. **Martinelli C, Pucci C and Ciofani G** (2019) Nanostructured carriers as innovative tools for cancer diagnosis and therapy. *APL Bioengineering* **3**, 011502.

8. **Senapati S, Mahanta AK, Kumar S and Maiti P** (2018) Controlled drug delivery vehicles for cancer treatment and their performance. *Signal Transduction and Targeted Therapy* **3**, 7.

9. **Hossen S, Hossain MK, Basher MK, Mia MNH, Rahman MT and Uddin MJ** (2019) Smart nanocarrier-based drug delivery systems for cancer therapy and toxicity studies: a review. *Journal of Advanced Research* **15**, 1–8.

10. **Liu Y and An X** (2019) Preparation, microstructure and function of liposome with light responsive switch. *Colloids Surfaces B* **178**, 238–244.

11. **Nardoni M, Della Valle E, Liberti M, Relucenti M, Casadei M, Paolicelli P, Apollonio F and Petralito S** (2018) Can pulsed electromagnetic fields trigger on-demand drug release from high-tm magnetoliposomes? *Nanomaterials* **8**, 196, 1–9.

12. **Kim K and Lee WG** (2017) Electroporation for nanomedicine: a review. *Journal of Materials Chemistry B* **5**, 2726–2738.

13. **Akbarzadeh A, Rezaei-sadabady R, Davaran S, Joo SW and Zarghami N** (2013) Liposome: classification, preparation, and applications. *Nanoscale Research Letters* **8**, 1–9.

14. **Retelj L, Pucihar G and Miklavcic D** (2013) Electroporation of intracellular liposomes using nanosecond electric pulses – a theoretical study. *IEEE Transactions on Biomedical Engineering* **60**, 2624–2635.

15. **Denzi A, Camera F, Merla C, Benassi B, Consales C, Paffi A, Apollonio F and Liberti M** (2016) A microdosimetric study of electropulsation on multiple realistically shaped cells: effect of neighbours. *The Journal of Membrane Biology* **249**, 691–701.

16. **Casciola M, Liberti M, Denzi A, Paffi A, Merla C and Apollonio F** (2017) A computational design of a versatile microchamber for in vitro nanosecond pulsed electric fields experiments. *Integration VLSI Journal* **58**, 446–453.

17. **Paffi A, Pellegrino M, Beccherelli R, Apollonio F, Liberti M, Platano D, Aicardi G and D'Inzeo G** (2007) A real-time exposure system for electrophysiological recording in brain slices. *IEEE Transactions on Microwave Theory and Techniques* **55**, 2463–2481.

18. **Liberti M, Apollonio F, Paffi A, Pellegrino M and D'Inzeo G** (2004) A coplanar-waveguide system for cells exposure during electrophysiological recordings. *IEEE Transactions on Microwave Theory and Techniques* **52**, 2521–2528.

19. **Paffi A, Banin A, Denzi A, Casciola M, Liberti M and Apollonio F** (2019) Broadband coplanar system for in vitro experiments, 2019 European Microwave Conference in Central Europe (EuMCE), Prague, Czech Republic, pp. 639–642.

20. **Merla C, Liberti M, Marracino P, Muscat A, Azan A, Apollonio F and Mir LM** (2018) A wide-band bio-chip for real-time optical detection of bioelectromagnetic interactions with cells. *Scientific Reports* **8**, 1–13.

21. **Casciola M, Xiao S, Apollonio F, Paffi A, Liberti M, Muratori C and Pakhomov AG** (2019) Cancellation of nerve excitation by the reversal of nanosecond stimulus polarity and its relevance to the gating time of sodium channels. *Cellular and Molecular Life Sciences* **76**, 4539–4550.

22. **Paffi A, Apollonio F, Lovisolo GA, Marino C, Pinto R, Repacholi M and Liberti M** (2010) Considerations for developing an RF exposure system: a review for in vitro biological experiments. *IEEE Transactions on Microwave Theory and Techniques* **58**, 2702–2714.

23. **Kenaan M, Amari SE, Silve A, Merla C, Mir LM, Couderc V, Arnaud-Cormos D and Leveque P** (2011) Characterization of a 50-Ω exposure setup for high-voltage nanosecond pulsed electric field bioexperiments. *IEEE Transactions on Biomedical Engineering* **58**, 207–214.

24. **Silve A, Vézinet R and Mir LM** (2012) Nanosecond-duration electric pulse delivery in vitro and in vivo: experimental considerations. *IEEE Transactions on Instrumentation and Measurement* **61**, 1945–1954.

25. **DeBruin KA and Krassowska W** (1999) Modeling electroporation in a single cell. I. Effects of field strength and rest potential. *Biophysical Journal* **77**, 1213–1224.

26. **Mercadal B, Vernier PT and Ivorra A** (2016) Dependence of electroporation detection threshold on cell radius: an explanation to observations non compatible with Schwan's equation model. *Journal of Membrane Biology* **249**, 663–676.

27. **Neu JC and Krassowska W** (1999) Asymptotic model of electroporation. *Physical Review E* **59**, 3471–3482.

28. **Krassowska W and Filev PD** (2007) Modeling electroporation in a single cell. *Biophysical Journal* **92**, 404–417.

29. **Orlacchio R, Carr L, Palego C, Arnaud-Cormos D and Leveque P** (2021) High-voltage 10 ns delayed paired or bipolar pulses for in vitro bioelectric experiments. *Bioelectrochemistry (Amsterdam, Netherlands)* **137**, 107648.

30. **Pakhomov AG, Semenov I, Xiao S, Pakhomova ON, Gregory B, Schoenbach KH, Ullery JC, Beier HT, Rajulapati SR and Ibey BL** (2014) Cancellation of cellular responses to nanoelectroporation by reversing the stimulus polarity. *Cellular and Molecular Life Sciences* **71**, 4431–4441.

31. **Lamberti P, Romeo S, Sannino A, Zeni L and Zeni O** (2015) The role of pulse repetition rate in nsPEF-induced electroporation: a biological and numerical investigation. *IEEE Transactions on Biomedical Engineering* **62**, 2234–2243.

32. **Merla C, Denzi A, Paffi A, Casciola M, D'Inzeo G, Apollonio F and Liberti M** (2012) Novel passive element circuits for microdosimetry of nanosecond pulsed electric fields. *IEEE Transactions on Biomedical Engineering* **59**, 2302–2311.

33. **Merla C, Liberti M, Apollonio F and D'inzeo G** (2009) Quantitative assessment of dielectric parameters for membrane lipid bi-layers from rf permittivity measurements. *Bioelectromagnetics* **30**, 286–298.

34. **Caramazza L, De Angelis A, della Valle E, Denzi A, Nardoni M, Paolicelli P, Petralito S, Apollonio F and Liberti M** (2019) Numerical

investigations of CW electric fields on lipid vesicles for controlled drug delivery, 2019 49th European Microwave Conference (EuMC), Paris, France, pp. 220–223.

35. **Hanna H, Denzi A, Liberti M, André FM and Mir LM** (2017) Electropermeabilization of inner and outer cell membranes with microsecond pulsed electric fields: quantitative study with calcium ions. *Scientific Reports* **7**, 13079.
36. **Li H, Denzi A, Ma X, Du X, Ning Y, Cheng X, Apollonio F, Liberti M and Hwang JCM** (2017) Distributed effect in high-frequency electroporation of biological cells. *IEEE Transactions on Microwave Theory and Techniques* **65**, 3503–3511.
37. **Foster KR and Schwan HP** (1986) *Handbook of Biological Effects of Electromagnetic Fields*. Boca Raton, FL: CRC Press.

Laura Caramazza received a master's degree (*cum laude*) in Nanotechnology Engineering at the Sapienza University of Rome in 2018. Presently, she is at the beginning of the third year of the Ph.D. in Information and Communications Technologies (curriculum Electronic Engineering), at the Sapienza University of Rome and supported by the Center for Life Nano Science of Istituto Italiano di Tecnologia (IIT), Rome, Italy. Her research topic is focused on the study of drug delivery systems activated by electric and magnetic fields. She has an active part in the collaboration with the Department of Drug Chemistry of Sapienza University. She worked at the CNRS – University of Paris-Saclay – Gustave Roussy UMR 9018, METSY, Paris, France during her Short Term Mission as Grant winner for the project "Investigations on driving mechanisms of lipid vesicles destabilization due to intense electric fields with characteristics of the lightning" in the framework of the COST Action [CA15211] ElectroNET.

Alessandra Paffi received the Laurea degree (*cum laude*) in the Department of Electronic Engineering and the doctorate from the Sapienza University of Rome, Rome, Italy. From 2011 to 2014, she was an Assistant Professor with the Department of Information Engineering, Electronics and Telecommunications (DIET) of the same university. She is a current postdoctoral fellow with the Italian Inter-University Center of Electromagnetic Fields and Biosystems (ICEmB) and a contract professor of "Electromagnetic compatibility for biomedical apparatuses" and "Processing of biomedical data and signals II" for the Biomedical Engineering Course of the Sapienza University of Rome. Her main research interests include theoretical and experimental studies for modeling interactions between electromagnetic fields and biological systems. Special interest is devoted to the design and fabrication of *in vitro* and *in vivo* exposure systems.

Micaela Liberti received the M.Sc degree in the Department of Electronic Engineering and the doctorate from the Sapienza University of Rome, Italy in 1995 and 2000, respectively. She is currently an Associate Professor with the Department of Electronic Engineering, Sapienza University. Presently, she is the President Elect of the European Bioelectromagnetic Association (EBEA) that she joined as a Scientific Council member first and Secretary afterward since 2008. From 2018 to 2019, she has been Technical Program Committee Chair of the Bioelectromagnetics Conference. Since 2018 she is an Associate Editor in the editorial board of the IEEE Journal of Electromagnetics, RF, and Microwaves in Medicine and Biology, and since 2016 she acts as a Review Editor for Frontiers in Public Health–Radiation and Health. From 2012 to 2015, she served as the national supplent representative of COST TD1104: "European network for development of electroporation-based technologies and treatments". From 2008 to 2012, she has been an expert member in the Coordinated Action COST BM0704 "Emerging EMF Technologies Health Risk Management" and from 2004 to 2008, she has been an expert member of the Technical Working Groups in the EMF-NET "Effects of the exposure to electromagnetic fields: From science to public health and safer workplace", 6th Framework Program. Her scientific interests include theoretical modeling in bioelectromagnetics, microdosimetry, exposure systems dosimetry and design, biomedical applications of EM fields, electroporation.

Francesca Apollonio (M'06) received the doctorate from the Sapienza University of Rome, Rome, Italy, in 1998. Since 2000, she joined the Department of Electronic Engineering, the Sapienza University of Rome as an Assistant Professor and since 2019 she is an Associate Professor. Presently, she is Chair of the National Commission CNR-URSI, Commission K "Electromagnetics in Biology and Medicine", while she has been a member of the same Commission since 2011. Since 2016 she has been a National Representative for the Action COST CA15211: "Atmospheric Electricity Network: coupling with the Earth System, climate and biological systems" (Electronet). From 2012 to 2015, she served on the Board of Directors of the Bioelectromagnetic Society. In 2015 and 2016, she has been Chair of the TPC (Technical Program Committee) for the Annual Meeting of the Bioelectromagnetics Society (BEMS) and the European BioElectromagnetics Association (EBEA), BioEM2016 held in Ghent, Belgium. Her research interests include the main aspects related to the interaction between electromagnetic fields and biological systems using both theoretical and experimental approaches, with particular reference to keywords as electroporation, smart drug delivery, molecular simulations of complex systems, and implantable and wearable medical devices.